International Journal of Thermofluids 22 (2024) 100598

Contents lists available at ScienceDirect

International Journal of Thermofluids

journal homepage: www.sciencedirect.com/journal/international-journal-of-thermofluids

Performance assessment of ISO-5167 and symmetrical Venturi meters for measuring low Reynolds number turbulent incompressible isothermal flow

Ahmad Sharifian *, Keith Wells

School of Engineering, University of Southern Queensland, Darling Heights QLD 4350, Australia

ARTICLE INFO

Keywords:
Venturi flow meter
Beta-ratio (β)
Convergent cone angle
Divergent cone angle
Pressure loss
Relative pressure loss coefficient (ζ)
Discharge coefficient (Cd)

ABSTRACT

The selection of Venturis depends on the desired flow measurement sensitivity, permanent pressure loss, discharge coefficient, and relative pressure loss coefficient. The ISO-5167 standard specifies geometries for Venturi metres within the Reynolds number range of 200,000 to 2,000,000. This study evaluates the performance of ISO-5167 and six suggested symmetrical Venturis operating in both unidirectional and bidirectional flow conditions for flows with Reynolds numbers below 200,000. The performance of ISO-5167 and six suggested symmetrical Venturis with β-ratios of 0.4 and 0.55, and cone angles of 10°, 20°, and 40° degrees were evaluated. The study found that the ISO-5167 Venturi performed best in the conventional flow direction for flows with Reynolds numbers greater than ≈34,000. The symmetrical Venturi meter with a β-ratio of 0.55 and a cone angle of 10° (SVD4) exhibited performance comparable to the ISO-5167 Venturi for the conventional flow direction. The ISO-5167 Venturi exhibited a significant flow reversal when operating in the opposite direction to the conventional flow. The SVD4 Venturi metre demonstrated the potential to save 71 % of energy in the reverse flow direction compared to the ISO-5167 Venturi, suggesting an energy saving of up to 43 % in certain bi-directional flow scenarios.

1. Introduction

The Venturi flow meter operates on the principle of differential pressure and is one of the oldest methods of measuring flow. The Venturi recovers approximately 90 % of the pressure drop, can measure the flow rate of an extensive range of fluids, and contains no moving parts. The Venturi meter is appropriate for high-velocity, high-pressure, and high-temperature applications. It is suitable for bidirectional flow applications and is not prone to sediment build-up [1]. Research by Reader-Harris [2] suggests that a significant advantage of the Venturi meter is that it allows the discharge coefficient to be calculated rather than measured, which may eliminate the need for calibration, providing the Venturi meter is manufactured to a standard.

According to the guidelines outlined in ISO-5167-part 4 standard [3], the initial stage in calculating the permanent pressure loss through a Venturi meter involves the installation of a constant diameter tube with matching length, diameter (D), and surface roughness to that of the Venturi meter. Once the equivalent length tube is installed, the inlet ($P_{1,\,TUBE}$) and outlet ($P_{3,TUBE}$) pressures are measured. Next, the Venturi is tested by measuring the inlet pressure ($P_{1,\,VEN}$), outlet pressure ($P_{3,\,VEN}$), and pressure at the throat ($P_{2,\,VEN}$). The permanent pressure loss due to the Venturi effect is then calculated using the measured pressure values and Eq. (1).

$$\text{Permanent pressure loss} = \left(P_{1,\text{VEN}} - P_{3,\text{VEN}}\right) - \left(P_{1,\text{TUBE}} - P_{3,\text{TUBE}}\right) \tag{1}$$

The sensitivity of a Venturi meter and the measurement accuracy increase as the pressure difference between the inlet and the throat increases. This pressure difference heavily depends on the β-ratio, which is the ratio of the throat diameter to the inlet diameter [4]. In most applications, a Venturi with the lowest relative pressure loss coefficient (ζ) (see Eq. (2)) is desirable [3]. This ratio provides a metric for evaluating energy loss and flow measurement accuracy and is a decisive criterion for selecting a Venturi meter.

$$\zeta = \frac{\left(P_{1,\text{VEN}} - P_{3,\text{VEN}}\right) - \left(P_{1,\text{TUBE}} - P_{3,\text{TUBE}}\right)}{P_{1,\text{VEN}} - P_{2,\text{VEN}}} = \frac{\Delta P_{permanent}}{P_{1,\text{VEN}} - P_{2,\text{VEN}}} \tag{2}$$

The discharge coefficient (Cd) of a Venturi meter is defined in Eq. (3).

* Corresponding author.
E-mail address: sharifia@usq.edu.au (A. Sharifian).

https://doi.org/10.1016/j.ijft.2024.100598

Available online 8 February 2024

$$Q = C_d \sqrt{\frac{2\left(P_{1,VEN} - P_{2,VEN}\right)}{\rho_1}} \frac{A_D}{\sqrt{\left(\frac{A_D}{A_d}\right)^2 - 1}} \quad (3)$$

Where Q is volume flow rate, C_d is discharge coefficient, $P_{1,VEN}$ is inlet pressure, $P_{2,VEN}$ is the pressure at the throat, ρ_1 is the density of the fluid at the inlet, A_D is the cross-sectional area of Venturi entry, and A_d is the cross-sectional area of the throat.

The specific applications of the Venturi flow meter vary significantly due to the flow rate requirements, the fluid type, and the Reynolds number (*Re*). Previous research recommends several different β-ratios between 0.2 to 0.8 to lower the energy loss [5], which is also sensitive to changes in the recovery cone angle. Existing research on Venturi flow meter design suggests that acceptable divergent cone angles between 7° and 15° can help reduce energy loss and potential flow separation [6]. The Venturi meter geometry is a key factor influencing flow separation, which determines the Reynolds number and the pressure gradient. At Reynolds numbers between approximately 200,000 and 1,000,000, the flow through the Venturi is turbulent, the effect of the static-hole error is relatively predictable, and the level of uncertainty is reasonably low. However, for *Re* values above 1,000,000, the static-hole error is unpredictable, and the level of uncertainty increases [2].

The most used standards for Venturis are ISO-5167 and ASME MFC-14M. While both standards aim to provide accurate and reliable flow measurements with minimal pressure loss, resulting in many similarities, there are some differences in their specifications and requirements. This study selected the ISO-5167 Venturi meter due to its well-defined guidelines for measuring pressure loss. The specifications described in the ISO-5167 standard are for asymmetrical cone angle geometry, optimised for unidirectional turbulent flow conditions operating with Reynolds numbers greater than 200,000. However, depending on the required consumption, Venturis designed for high Reynolds numbers may also encounter low Reynolds flows. Furthermore, there are situations where the Reynolds number range is less than 200,000, such as lines containing high-viscosity fluid, pipes with small diameters and low-velocity applications. In industry, most flow conditions are unidirectional. However, the unidirectional reverse flow condition also requires consideration. In bidirectional flow systems, such as artificial respiration lines, water pipes between several treatment plants, steam lines between two units in a plant, the pumping of dielectric fluid for cooling underground high-voltage electrical cables and pipes for injecting or withdrawing gas from the field, precise flow measurement with low energy loss is desirable. In such applications, it is desirable to have a Venturi that can accurately measure the flow rate with minimal losses in both directions. This highlights the significance of a symmetrical Venturi, capable of functioning in both flow directions with low loss and governed by a single formula that relates the measured pressure differential to the volume flow rate. The application of the Venturi effect is not restricted solely to flow measurement. It has been employed to increase velocity and/or drop pressure at its throat. For example, it has been utilised to enhance the performance of wind delivery systems to wind turbines [7–10], Venturi scrubbers for liquid atomisation [11], and in increasing the efficiency of marine organic Rankine cycle units [12].

This study aimed to assess the performance of ISO-5167 Venturi meters and identify a suitable Venturi for applications in low Reynolds turbulent flow ($Re < 200{,}000$) and/or bidirectional scenarios. The research focused on analysing the performance of six designed symmetrical Venturi meters concerning flow measurement sensitivity, permanent energy loss, discharge coefficient, and relative pressure loss coefficient. These performance metrics were compared against the Venturi meter described in the ISO-5167 standard.

2. Background

It is well known that in the convergent section of a Venturi meter, the flow experiences a decrease in pressure in the flow direction. The accelerated flow results in the boundary layer becoming thinner, meaning the fluid flow is closer to the surface of the meter, ensuring flow stability and reducing turbulence [13]. This concept is consistent with the research of Liu et al. [14], who demonstrated that negative pressure gradients suppress flow separations. The convergent angle can be relatively large since the convergent section is not prone to flow separation.

The divergent section of a Venturi meter significantly affects energy loss [15]. Pipe flow regions where the cross-sectional area increases are vulnerable to flow separation. When fluid flow experiences an increasing pressure gradient, the fluid outside the boundary layer has enough momentum to overcome the pressure trying to push against it. However, the fluid momentum within the boundary layer is small and can reverse when trying to overcome the pressure in the divergent section, causing flow separation [13]. A study [16] concluded that for divergent cone angles less than 7°, flow separation does not occur. A study by White [17] indicates that angles greater than 15° can result in flow separation for the Reynolds number range 150,000 to 2,000,000. An explanation for the difference in the divergent cone angle is presented in the research of Sparrow et al. [15], who suggested that flow separation also depends on the Reynolds number.

In a study [18], the Taguchi method was employed for the design of the CFD analysis, offering a systematic approach to identify the combinations of parameters that have the most significant impact on energy loss. The identified input variables were the convergent cone angle (θ_1), divergent cone angle (θ_2), β value, throat diameter (d) and throat length (l), with the output parameter being the permanent pressure loss. The research did not specify the Reynolds number range. The results from the study identified an optimal Venturi geometry as having a convergent cone angle of $\theta_1 = 34°$, a divergent cone angle of $\theta_2 = 14°$, a β-ratio of 0.75 and a throat diameter $d = 7$ mm. The study [18] suggested that the β-ratio has the highest impact on permanent pressure loss, followed by throat length, convergent cone angle and divergent cone angle.

An experimental study [4] shows the effect of the *Re* on the Cd for β-ratios of 0.3, 0.5 and 0.7. The study [4] results indicate that an increase in the Re leads to an increase in Cd for β-ratios of 0.3, 0.5 and 0.7 in the approximate Reynolds number ranges 5000–32,000, 10,000–60,000 and 31,000 to 65,000, respectively. Another finding was that Cd varied abruptly for the lower *Re* values previously mentioned for the β values 0.3 and 0.5, becoming more predictable as the *Re* increased. The reasoning proposed by authors [4] for the fluctuations at low *Re* values was due to the parabolic velocity profile and the associated viscous effects.

Another finding of the study [4] was the impact of the variation of the β-ratio on the average value of the Cd. The research demonstrated that the value of the Cd decreases as the β increases when taking the average of the near-constant values of the Cd and the *Re*. The decrease in Cd increases significantly between the β-ratios of 0.5 and 0.7. The highest average value for Cd was 0.96, which occurred at the β-ratio of 0.3.

Kaladgi et al. [4] demonstrated that a β of 0.3 experienced a pressure drop of 81.8 % between the inlet and the throat section, a β of 0.5, 14.1 % and a β of 0.7, a 2.7 % pressure drop. Although these pressure drops were essential for flow measurement, the study indicated that the pressure regained in the divergent section was not equal to the pressure of the pipe inlet, which confirms that significant energy losses certainly occur for the β-ratios of 0.3, 0.5 and 0.7 in the previously mentioned *Re* ranges.

The ISO-5167 standard specifies that Venturi meters, when manufactured according to the prescribed geometrical and dimensional requirements, can achieve a ζ of around 0.04 to 0.16 for Reynolds numbers greater than 1,000,000 and a β-ratio range of 0.3 to 0.75. For a β-ratio of 0.55, the estimated ζ falls within the range of 0.07 to 0.13, with slight variation observed for *Re* values above 1,000,000. The standard suggests that the discharge coefficients and uncertainties remain relatively constant for *Re* values above 2,000,000 [3]. A considerable number of

studies have described the performance of Venturi meters at *Re*ynolds numbers where ζ, Cd, and uncertainty reach a stable state [4]. However, limited research is available for Reynolds numbers below 1,000,000, highlighting the need to investigate lower Reynolds numbers, as carried out in this study.

3. Methodology

This study addresses the aforementioned research gaps using computational and experimental approaches. The scope of this study is limited to six 50 mm symmetrical Venturi meters (SVD1-SVD6) and one asymmetrical Venturi meter (ISO-5167) designed and printed in transparent stereolithography (SLA) resin. The throat length for each Venturi was equal to the throat diameter. Simulations were conducted on each meter using water as the fluid and at an inclination of 0°

3.1. Experimental approach

3.1.1. Experimental setup

Fig. 1 presents the experimental setup consisting of seven Venturi meters mounted at a 0° inclination angle, a pump, pump controller, PVC pipes, tubes, an accumulator, drain, recycle tanks, and three pressure gauges.

A pump with a flow capacity of 150 L/min provided the water for experimentation, with the water pressure regulated by a pump controller. The water was stored in a 1000 L recycle tank. A 50 mm ball valve tap was installed in the supply pipe to the pump to control the flow rate. Although the pump controller allowed some adjustments, the available flow parameters were limited by the maximum pressure and flow rate capacity of the pump, resulting in a restricted Reynolds number range during experimentation.

Seven Venturi meters were designed in Autodesk Fusion 360 and ANSYS Fluent and then printed in transparent SLA resin. One Venturi meter was designed to specifications prescribed in the ISO-5167 standard, and the other six Venturi meters had symmetrical cone angles. The SLA resin Venturi meters had post-processing techniques applied to the internal surface to ensure a roughness (e) value of 2 μm was achieved, which aligned with the prescribed specifications in the ISO-5167 standard. Table 1 presents the main parameters of each Venturi meter, and Fig. 2 shows the geometry details.

According to the ISO-5167 standard [3], the inlet and outlet pressure tappings should be located at a minimum distance of D (inlet diameter) upstream and 6D downstream of the inlet and outlet flanges, respectively. The Venturi meters in this study had a fixed inlet diameter (D) of 50 mm, resulting in an upstream length of 50 mm and a downstream length of 300 mm. Furthermore, the lengths of straight pipes upstream of the inlet tapping and downstream of the outlet tapping are 1419 mm and 536 mm, respectively. Additionally, there should be a minimum of four pressure tappings for the throat, as shown in Fig. 3a and b. Fig. 3c depicts the recycling system (1000 L) and the measurement tank (35 L) used to measure the flow rate.

3.1.2. Experimental uncertainties

The experimentation was conducted for six consecutive days in ambient temperatures ranging from 13 °C to 24 °C. All the experimental results presented are the averages of at least 15 readings obtained within this temperature range. The average temperature of the readings for each Venturi measurement slightly differed and was evaluated as 18 °C ± 1 °C. This average temperature variation introduced an uncertainty of ±2.6 % in the viscosity calculation and Reynolds number and 0.1 % in the density calculation.

The water used for the experimentation was sourced from the town water supply and stored in a 1000 L recycle tank. Throughout the experiments, the water level in the recycle tank was consistently maintained at approximately 500 L. A 35 L flow measurement tank (Fig. 3c) and a stopwatch were employed to measure the flow rate in each experiment, with no discernible differences observed in the flow rate across the various experiments. The response time of an operator is dependent on factors such as their attention level, age, and other variables. In this study, an average response time of ±0.5 s was assigned to the operator. The flow rate maintained throughout the experiments was 1.33 L/s, resulting in an uncertainty of ±2 %. Considering the 2.6 % uncertainty due to viscosity measurement errors, the overall uncertainty in the Reynolds number was estimated to be 3.3 %, or Re = 33,754 ± 1100. The experiments yielded a calculated Reynolds number of 33,754, which was used for computational modelling. However, to account for

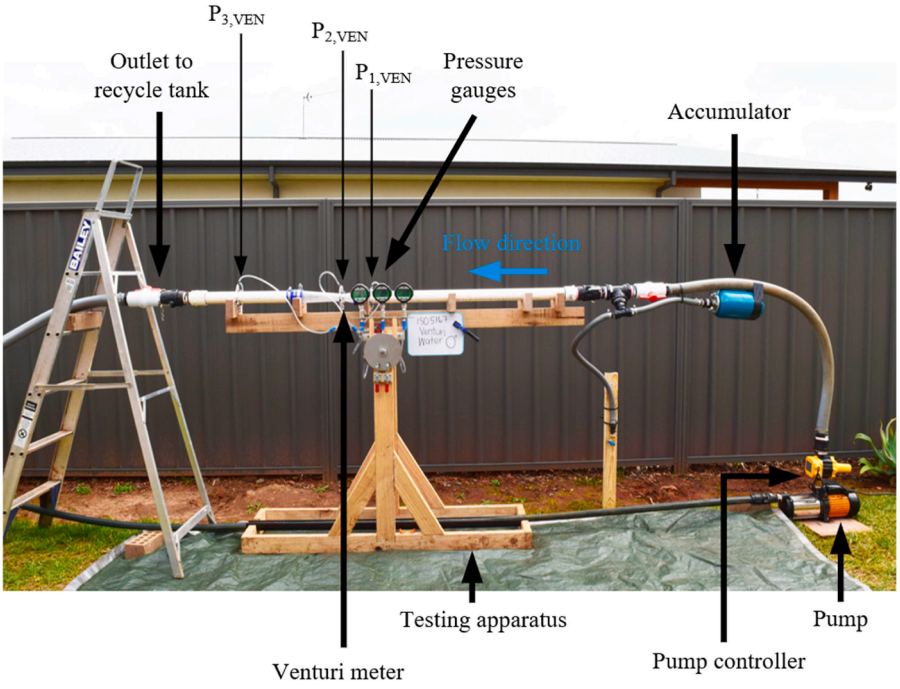

Fig. 1. Experimental setup at an inclination angle of 0°.

Table 1
Venturi flow meter specifications. Inlet and outlet diameters for all Venturis are 50 mm.

Venturi	β	Throat Length= Throat diameter (mm)	Convergent/divergent cone angle	Venturi convergent length (mm)	Venturi divergent length (mm)	Venturi length (mm)	Distance between inlet and outlet tappings (mm)
SVD1	0.40	20	10°/10°	171.45	171.45	392.9	742.9
SVD2	0.40	20	20°/20°	85.07	85.07	220.14	570.14
SVD3	0.40	20	40°/40°	41.21	41.21	132.42	482.42
SVD4	0.55	27.5	10°/10°	128.59	128.59	314.68	664.68
SVD5	0.55	27.5	20°/20°	63.80	63.80	185.1	535.1
SVD6	0.55	27.5	40°/40°	30.91	30.91	119.32	469.32
ISO-5167	0.55	27.5	21°/7°	60.70	183.94	302.14	652.14

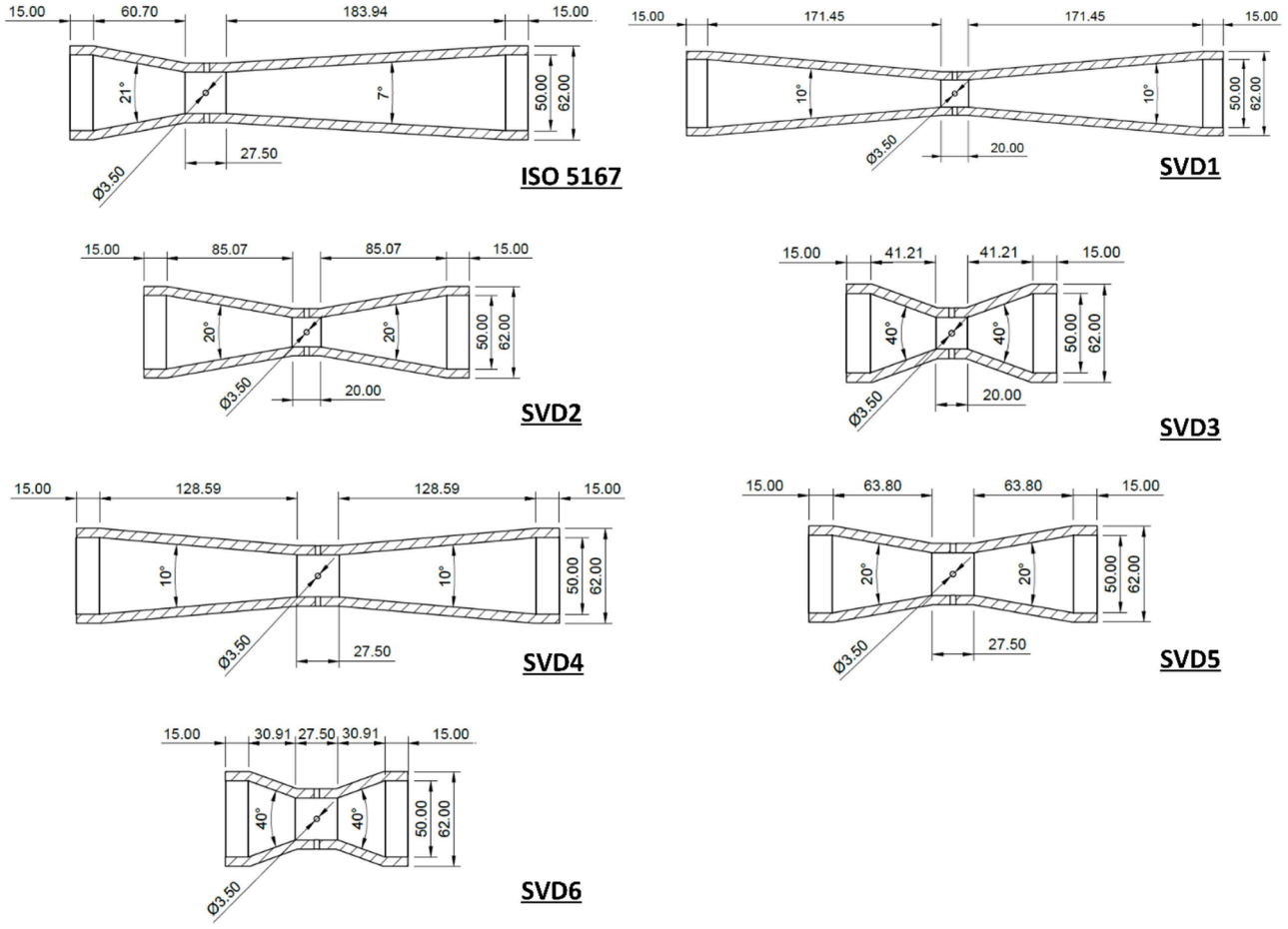

Fig. 2. The detailed geometries of the seven Venturis employed in this work.

combined uncertainties, the value was presented as $Re \approx 34{,}000$ in this study.

The digital angle meter used to set the Venturi mounting angle to 0° of inclination was factory calibrated to ±0.2° and regularly checked (at 0° and 90°) using a water level. Another water level was installed on the testing apparatus frame to ensure the experimentation occurred on level ground. Considering the relatively short length of each Venturi, the precision of angle measurement caused a minor uncertainty of up to 0.1 Pa.

The manufacturer specified the accuracy of the Easyelec model 220,110 pressure gauges as ±0.02 % on a full scale of 30 kPa, resulting in an uncertainty of ±6 Pa. The pressure gauge has a response time of 8 ms and operates within a temperature range of −40 °C to 80 °C. Additionally, it features automatic correction for temperature drift. However, the gauges only had a resolution of 10 Pa, leading to a measurement uncertainty of ±10 Pa. Additionally, the uncertainty of the permanent pressure loss ($\Delta P_{1\text{-}3} = P_1\text{-}P_3$) and the pressure differential between the inlet and throat ($\Delta P_{1\text{–}2} = P_1\text{-}P_2$) for both the Venturis and the PVC tubes is estimated to be ±14 Pa. Considering the reported pressure differences are the difference of $\Delta P_{1\text{–}2}$ and $\Delta P_{1\text{–}3}$ of Venturis and those of PVC tubes, the experimental uncertainties are estimated to be ±20 Pa.

3.2. Computational approach

3.2.1. Computational modelling

The Venturi meters were modelled using axisymmetric geometry. However, axisymmetric modelling did not allow for the investigation of gravity and pressure tapping points. This is not expected to impact the results significantly, considering all Venturis are oriented horizontally, and the height differences between the top and bottom tappings are

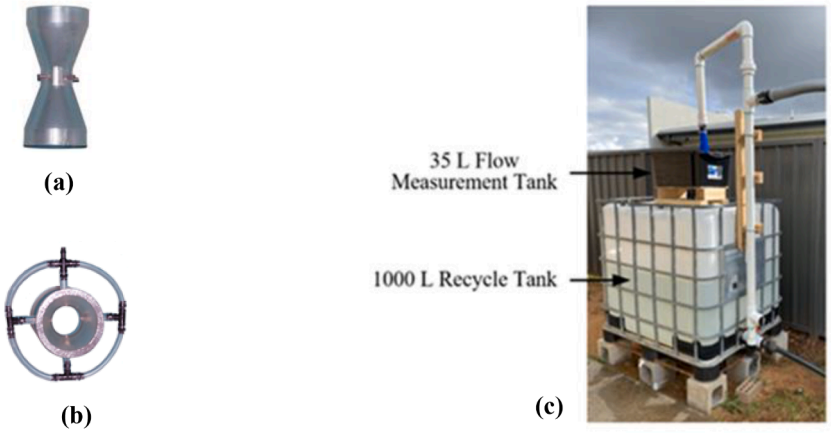

Fig. 3. Venturi manifold tappings and flow measurement system, a) Front view of Venturi and manifold tappings, b) Top view of Venturi manifold tappings, c) Measurement and recycle tanks.

minimal. Furthermore, in our experimental setup (refer to Fig. 3), the four tapping points were interconnected, allowing the measurement of the average pressure at each section. Adiabatic boundary conditions were used for the simulations, incorporating a specified water mass flow rate with a turbulent intensity of 5 % and a turbulent viscosity ratio of 10 at the inlet. The outlet boundary condition was a constant pressure, assuming backflow direction normal to the boundary, along with specified total pressure and backflow turbulent intensity of 5 % and viscosity ratio of 10. Additionally, a no-slip condition was applied at the walls. The roughness of the walls was 2 μm, with a roughness constant of 0.5. At a Reynolds number of ≈34,000, the inlet volume flow rate and the pressure at the outlet were identical values compared to the measured values. To achieve the desired Reynolds numbers, the inlet volume flow rate was adjusted. The variations in pressures along the Venturis remain unaffected by assumed outlet pressures, given the assumption of incompressible and isothermal water with constant properties. The computational domain extended from 1 times the inlet diameter (D) upstream of the Venturi's inlet flange to 6D downstream of the Venturi's outlet flange.

The mesh geometry used predominantly quadrilateral cells for the simulation, as recommended by several authors (e.g. [19]). The mesh generated for all Venturis and results were assessed using orthogonality, skewness and aspect ratio criteria. The average mesh orthogonal quality in all cases was greater than 0.97, with an average skewness of less than 0.15 and an average aspect ratio of less than 1.4. According to [20], these values indicate excellent mesh quality.

The Reynolds number for the experimental part of this study was ≈34,000, indicating that the flow conditions were in the mildly turbulent range. The CFD simulations utilised the Shear Stress Transport (SST) k-omega (k-ω) model. The chosen CFD simulation model uses two equations based on the Reynolds Averaged Navier Stokes (RANS) regime, which considers the effects of turbulence, and the results are generally more reliable [21]. The pressure-velocity coupling utilised the Rhio-Chow distance-based method, with solution control achieved through turbulent kinetic energy and a specific dissipation rate set at 0.75 per second. A second-order numerical method was employed for solving the governing equations.

3.2.2. *Verification of computational results*

Various measures were taken to ensure the accuracy and reliability of the computational results, including checking residuals, Grid Convergence Index (GCI), and Y^+. The continuity, velocity components, and turbulence residuals were below 10^{-8}. Additionally, a grid independence study was performed. To ensure consistency with experimental uncertainty, the pressure and pressure difference values (P_1-P_2) and (P_1-P_3) along the centreline were considered grid-independent when they exhibited changes of no more than 0.01 kPa, as observed by running the simulations multiple times with different mesh sizes. To ensure that the estimated error was sufficiently small, a target value of less than 5 % was set for the GCI with a safety factor of 1.25. A value of 5 % is commonly used as an indicator of good grid independence, while GCI values of up to 10 % have been successfully employed in previous research [22,23]. The value of Y^+ was carefully evaluated and aimed to be less than 5. While some studies have shown reliable results for Venturis with Y^+ values of around 10 to 30 [6], a study [24] recommends a Y^+ value of less than 5, with an optimal value of 1 for the SST k-ω turbulence model. Following these criteria, the steps for modelling the ISO-5167 Venturi are presented below.

Achieving residuals of less than 10^{-8} for the ISO-5167 Venturi required an element size of about 8 mm at the walls and a growth rate of 1.2 (totalling 320 elements). However, to achieve mesh independence, which results in a maximum pressure change of 0.01 kPa in two consecutive models, mesh sizes of approximately 0.15 mm at the walls were needed (totalling 250,531 elements). The grid convergence index (GCI), calculated using the formulas suggested by Roache [25] and others [26–28], was found to be 7 %. In order to achieve a GCI of 5 % or less, the element size needed to be reduced to 0.07 mm (395,100 elements). In this case, the value of Y^+ was 6.16 at some small areas of the wall.

The recommended Y^+ value of less than five was achieved by increasing the number of mesh elements to 513,551 and reducing the element size near the inlet and outlet of the throat to approximately 0.06 mm. An additional simulation with 677,887 elements (element size of about 0.03 mm at the walls near the inlet and outlet of the throat) was conducted to establish the ISO-5167 Venturi as a reference for other cases. This simulation resulted in a maximum Y^+ value of 3.32, reducing the GCI for (P_1-P_3) to 0.49 % and (P_1-P_2) to 0.01 % (GCI was calculated based on the modelling results with 395,100, 513,551, and 677,887 elements). Fig. 4 shows the mesh throughout the entire Venturi (Fig. 4a), the vicinity of the inlet to the throat (Fig. 4b), and the centreline pressure along the Venturi (Fig. 4c).

3.2.3. *Validation of computational results*

This study comprises a comprehensive computational work and some experimental work conducted at a Reynolds number of ≈34,000. The computational results were validated against the experimental results from this study and available data for ISO-5167 Venturi measurements.

The results of this study are consistent with the available results for the ISO-5167 Venturi. According to Appendix B of ISO-5167–4 [3], the discharge coefficient for the Classical Venturi ISO-5167 with an as-cast convergent section is 95.7 % ± 2.5 % at $Re = 40{,}000$ and 97.6 % ± 1.5 %

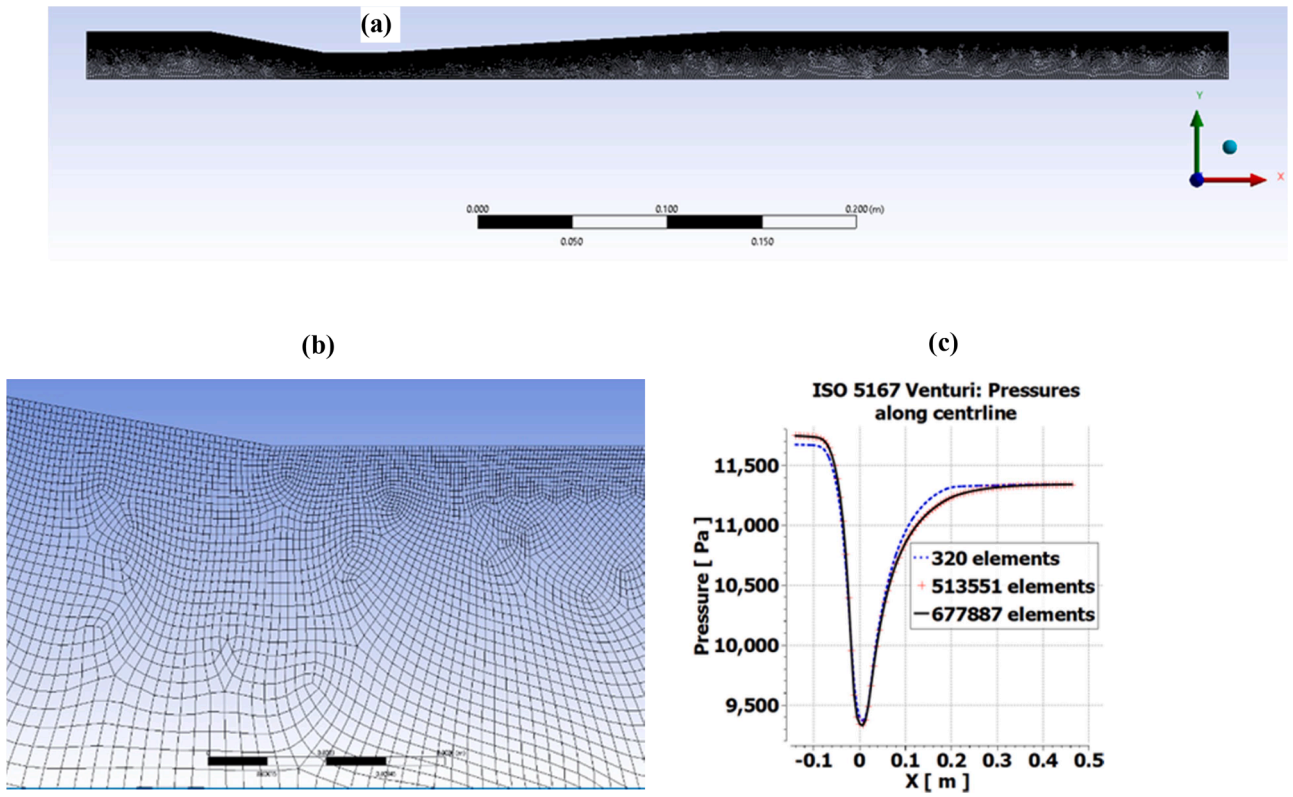

Fig. 4. Grids of ISO-5167 Venturi and mesh sensitivity tests, a) grids of the Venturi with 677,887 elements, b) grids around the inlet of the Venturi's throat, and c) computational pressures along the Venturi centreline using different numbers of elements.

at $Re = 100{,}000$. The value of Cd increases to 0.97, with an uncertainty of 3 %, for a classical Venturi tube with a machined convergent section and Reynolds number of 50,000. In this study, the discharge coefficients were 98 % at $Re = 34{,}000$, 50,000 and 100,000, which aligns with the results provided by the standard. According to Appendix C of the standard, the ζ value falls within the range of 0.07 to 0.16 for a β-ratio of 0.55 at $Re > 1000{,}000$. The standard also indicates that the ζ increases as the Reynolds number decreases. This study found $\zeta = 0.13$ at $Re = 34{,}000$, 0.13 at $Re = 50{,}000$, 0.11 at $Re = 100{,}000$, and 0.10 at $Re = 200{,}000$. These comparisons demonstrate that the Cd and ζ values fall within the range specified in the standard, and their changes with the Reynolds number are consistent with the predictions of the standard.

The validation process for the ISO-5167 Venturi, using the experimental results of this study, is described as follows. At a Reynolds number of ≈34,000, the computational and experimental values of ($P_{1,VEN}$-$P_{3,VEN}$) were 0.32 kPa and 0.31 kPa, respectively, with a difference of 0.01 kPa, which falls within the experimental uncertainty. However, the computational and experimental values of ($P_{1,VEN}$-$P_{2,VEN}$) were 2.38 kPa and 2.50 kPa, respectively, indicating a 5 % difference. The error in the measured pressure loss depends on several factors, including errors in pressure difference readings (0.02/2.38 = 0.8 %, see Section 3.1.2), errors in density measurement (0.1 %, see Section 3.1.2), errors in the friction factor, and twice the errors for volume flow rate, as pressure loss is related to the square of the volume flow rate (2 × 2 %= 4 %). It is important to note that some parts of the head loss (minor head loss) do not have a strong relationship with the Reynolds number; thus, this calculation is expected to show the maximum error. The Moody diagram and Darcy-Weisbach equation at Re≈34,000 were used to estimate the relationship between the friction factor and the Reynolds number. The data indicates that an error of 3.3 % at a Reynolds number of ≈34,000 can result in an approximate 5 % error in the friction factor. Therefore, the overall uncertainty can be estimated as $(0.8\,\%^2 + 0.1\,\%^2 + 5\,\%^2 + 4\,\%^2)^{0.5}$, which gives a 6.5 % uncertainty. Consequently, the difference of 5 % between the experimental and computational results can be justified in this case due to the overall estimated uncertainty of 6.5 %.

This study aimed to compare the performance of several Venturis. Notably, the order of Venturis based on computational and experimental permanent pressure losses and pressure changes from inlet to throat were identical, indicating reliable computational results. Therefore, it can be concluded that the obtained results were validated and fell within the acceptable tolerance range for the study.

4. Results

The CFD simulations and experimental data findings are presented and discussed in terms of flow patterns inside the Venturis, pressure losses, ζ, and Cd at Reynolds numbers of ≈34,000, 50,000, 100,000, and 200,000.

4.1. Flow patterns

The CFD simulations revealed that several Venturis exhibit reversed flow and vortices. As a result, the Venturis were categorised into three groups: those showing strong reversed flow, those at the threshold of reversed flow, and those without reversed flow.

The CFD simulations revealed pronounced reversed flow within the Venturis of SVD2, SVD3, SVD5, and SVD6. Fig. 5a and b illustrate the reversed flow within the SVD2 and SVD3 Venturis. The streamlines demonstrate that the SVD2 and SVD3 Venturis experienced reversed flow, which extends throughout the entire divergent section (see Fig. 5a & b). The combination of a low β-ratio (0.4) and high cone angles of 20° and 40° in these two Venturis results in the most significant reversed flow at a Reynolds number of ≈34,000. These Venturis were modelled at two Reynolds numbers of 5000 and 200,000, and the results indicated that the reversed flow persisted. At a Reynolds number of 200,000, the strength of the reversed flow increased, while at a Reynolds number of

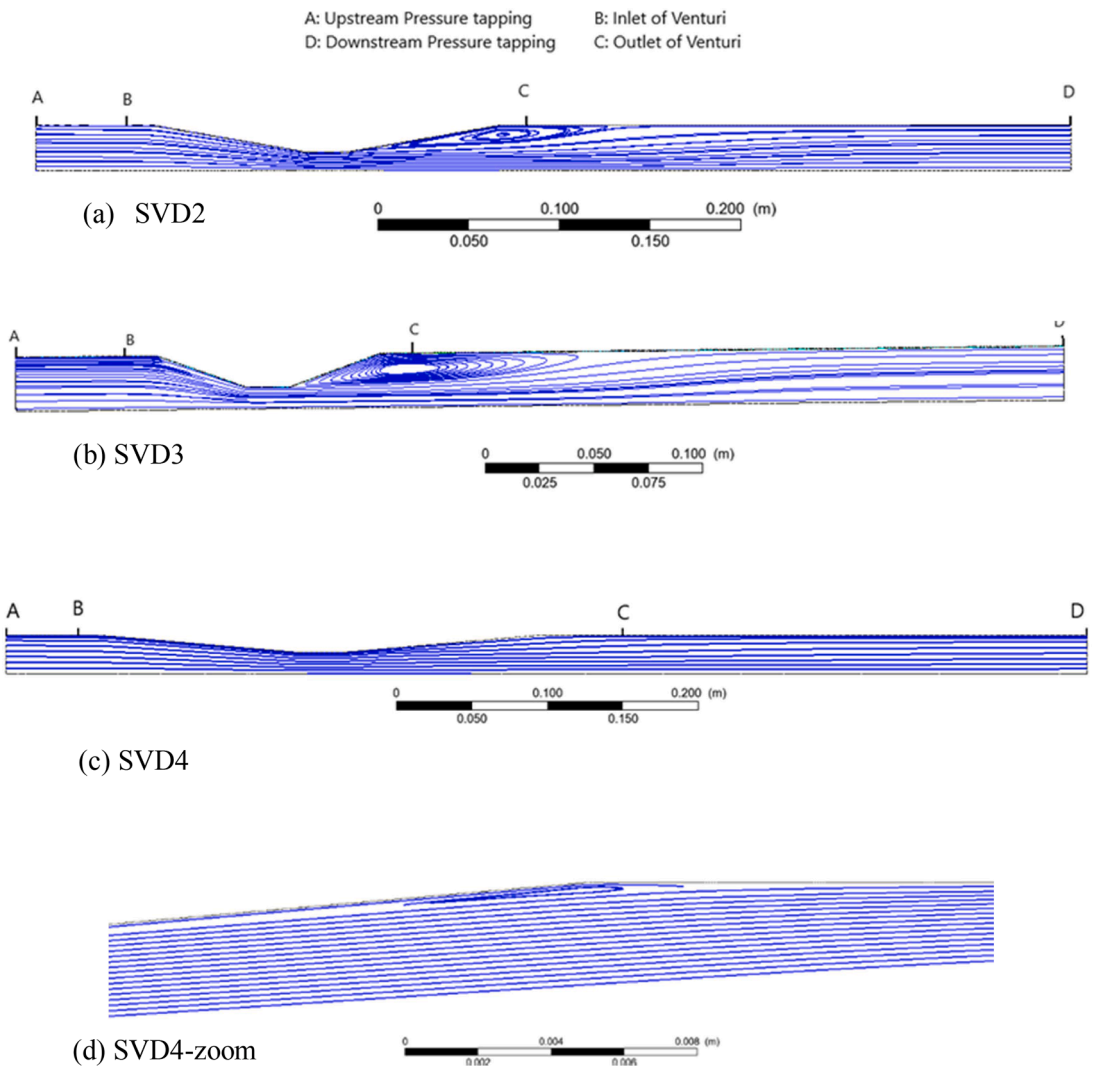

Fig. 5. Flow streamlines through multiple Venturis from left to right with a surface roughness of 2 μm at a Reynolds number of ≈34,000. The coordinate origin in all simulations is set at the middle of the throat: a) Venturi SVD2, b) Venturi SVD3, c) Venturi SVD4, and d) SVD4-zoom.

5000, the reversed flow was still present but weaker.

The SVD5 and SVD6 Venturis exhibited reversed flow, although to a lesser degree. These two Venturi meters have a β−ratio of 0.55, which is greater than the 0.40 β−ratio for SVD2 and SVD3 despite having the same cone angles.

The Venturis SVD1 and SVD4 were determined to be at the threshold of reversed flow, displaying some reversed flow in a limited section and exhibiting very low reversed velocities. Fig. 5c illustrates the flow within one of these Venturis, which appears to show parallel streamlines. However, upon closer investigation, it was found that they had a weak vortex at the end of their divergent section (see Fig. 5d for SVD4). The length of the vortex for SVD4 was approximately 10 mm, and its width was 0.5 mm (see Fig. 5d). This vortex exhibited a maximum reversed velocity of 10.6 mm/s. Although the Venturi SVD4 was at the threshold of reverse flow, the model results obtained for Reynolds numbers of 50,000, 100,000, and 200,000 revealed the absence of any reverse flow at Reynolds numbers greater than 100,000. Thus, the minimum Reynolds number at which this Venturi can be used without any reversed flow is approximately 100,000.

The ISO-5167 was the only Venturi meter examined in this study that did not demonstrate reversed flow at a Reynolds number of ≈34,000. The streamlines produced in the ISO-5167 appeared parallel, with no reversed flow detected at any point within the Venturi meter. Further computational work at Reynolds numbers 50,000, 100,000, and 200,000 also demonstrated no reversed flow. However, reversed flow was observed at a Reynolds number of 5,000 (see Fig. 6a). Furthermore, when the flow direction was changed, a strong, reversed flow was observed (refer to Fig. 6b). In that case, the reversed flow resulted in the formation of a vortex with a maximum velocity of 0.168 m/s that extended beyond the end of the Venturi (point C) and affected the flow pattern at the outlet pressure tapping point (point D), located at a distance D from the end of the Venturi.

4.2. Permanent pressure losses, relative permanent pressure loss and discharge coefficient

The Venturi meters of SVD1, SVD2, SVD3, SVD5, and SVD6 have been excluded from the list of suitable Venturis. This decision was made due to the presence of reversed flow and the generation of vortices. In accordance with Newton's shear stress law, reversed flow and vortices not only result in elevated shear stress and increased pressure losses but also introduce pressure fluctuations due to their transient nature. This, in turn, contributes to a higher degree of measurement errors. The SVD1 demonstrated reasonable performance and exhibited the highest-pressure measurement sensitivity, due to its low β−ratio. However, it was excluded from further consideration due to reversed flow at Reynolds numbers of 50,000, 100,000 and 200,000.

Table 2 presents the experimental and computational centreline

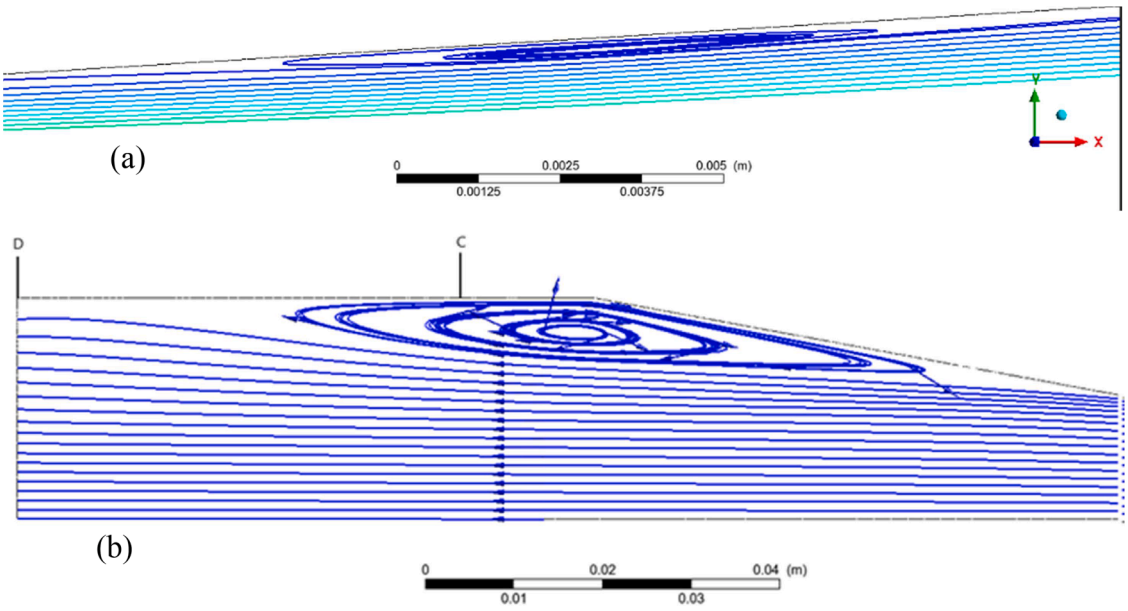

Fig. 6. Streamlines of flow through ISO-5167 Venturi with a surface roughness of 2 μm; a) flow at the conventional direction (left to right) at $Re = 5000$, and b) flow from right to left (reversed flow direction) at $Re = 34{,}000$.

Table 2
Experimental and computational results for Venturi meters with β-ratio of 0.55 ($Re \approx 34{,}000$, $e = 2$ μm).

Venturi	$P_{1,VEN}$ - $P_{2,VEN}$ (EXP.) (kPa)	$P_{1,VEN}$ - $P_{3,VEN}$ (EXP.) (kPa)	$P_{1,VEN}$ - $P_{2,VEN}$ (COMP.) (kPa)	$P_{1,VEN}$ - $P_{3,VEN}$ (COMP.) (kPa)	Cd (EXP.)	Cd (COMP.)	ζ (Exp.)	ζ (COMP.)
SVD4	2.44	0.38	2.42	0.41	0.97	0.98	0.16	0.17
ISO-5167	2.50	0.31	2.38	0.32	0.96	0.98	0.12	0.13

pressure differences for remaining symmetrical Venturis meters (SVD1) and the ISO-5167 Venturi at $Re \approx 34{,}000$.

Table 2 shows the performance of ISO-5167 and SVD4 Venturis at a $Re \approx 34{,}000$. The experimental results show the lower permanent loss and slightly higher measurement sensitivity (P_1-P_2) of Venturi ISO-5167 compared to SVD4. The computational results also demonstrate a similar trend to the experimental results, except for the order of measurement sensitivity. Although both Venturis have an identical β-ratio of 0.55, SVD4 has a lower cone angle (10°) compared to ISO-5167 (21°). Due to the higher convergent cone angle of ISO-5167, it was expected to show a higher (P_1-P_2). While the computational results confirm this expectation, the experimental results show otherwise. As a result, this study did not conclusively determine which one has higher measurement sensitivity at $Re \approx 34{,}000$. However, the computational and experimental work confirm that their measurement sensitivity is very similar.

Table 2 presents the experimental and computational discharge coefficients of the two Venturis. According to Eq. (3), the β−ratio influences the discharge coefficient (Cd) and (P_1-P_2). The results reveal that there is not a significant difference between the discharge coefficients of the two Venturis. It is essential to note that while having a high Cd would be ideal, it is not crucial in practice, as a lower permanent pressure loss between the inlet and throat of the Venturi meter does not necessarily translate to a lower pressure loss between the inlet and outlet of the Venturi, as is the case for the ISO-5167 Venturi.

The ζ defined in Eq. (2) represents a trade-off between measurement sensitivity and energy loss. Table 2 shows a good agreement between the computed and experimental ζ values. The results indicate that the ISO-5167 Venturi outperforms Venturi SVD4 in terms of the ζ ratio at a Reynolds number of approximately 34,000.

4.3. Performance of Venturis in the reverse direction of the flow

The performance of the ISO-5167 Venturi was simulated for flow in the reverse direction. However, there was no need for a separate study on the performance of the symmetrical Venturi SVD4 for reversed flow direction. The findings presented in Table 3 indicated that the ISO-5167 Venturi exhibited a robust reverse flow and vortex formation (see Fig. 6b) at a Reynolds number of ≈34,000. In this condition, the ISO-5167 Venturi had its inlet pressure tapping located at 6D upstream of the Venturi and the outlet pressure tapping at 1D downstream.

Table 3 illustrates a pressure drop of 2.47 kPa between the inlet pressure tapping and the middle of the throat, along with a permanent pressure loss of 1.41 kPa between the upstream and downstream pressure tapping points at $Re \approx 34{,}000$ for the ISO-5167 Venturi when the flow is reversed.

The permanent pressure loss of ISO-5167 at the reverse flow direction is almost 3.4 times that of SVD4. Additionally, the results show a very high ζ value of 0.57 compared to 0.17 for SVD4 in the case of reversed flow. These values and the existence of vortices indicate the low performance of the ISO-5167 Venturi for reversed flow at a Reynolds number of ≈34,000.

4.4. Performance of SVD4 and ISO-5167 Venturis at higher Reynolds number

The performance of the ISO-5167 Venturi in the conventional flow direction was ~~found to be~~ superior to the other six Venturi meters considered in this study at $Re \approx 34{,}000$. The SVD4 Venturi also performed relatively well at a $Re \approx 34{,}000$ in the conventional flow direction and outperformed ISO-5167 Venturi in the reversed flow. However, evaluating the performance of these two Venturis at different Reynolds numbers is essential to ensure the findings of the study are not limited to

Table 3
Comparison of the ISO-5167 and SVD4 Venturi flow meters using CFD results (e = 2 μm, Re = 34,000).

Venturi	Flow direction	β-ratio	Measurement sensitivity (kPa)	Permanent pressure loss (kPa)	ζ	Cd
ISO-5167 (21°/7°)	Conventional	0.55	2.38	0.32	0.13	0.97
SVD4 (10°/10°)	Conventional	0.55	2.42	0.41	0.17	0.97
ISO-5167 (7°/21°)	Reversed	0.55	2.47	1.41	0.57	0.96

a specific Reynolds number. Therefore, the two Venturis were modelled at Reynolds numbers of 50,000, 100,000, and 200,000 for both conventional and reverse flow directions, and the results are presented in Table 4.

The results for all three cases of ISO-5167C (conventional direction), ISO-5167R (reverse flow direction), and SVD4 follow the same pattern. In all cases, (P_1-P_2) and (P_1-P_3) increase as the Reynolds number increases. The performance of all three cases in terms of Cd and ζ improves when the Reynolds number increases. Additionally, all three cases show similar (P_1-P_2) as the β-ratio is identical (0.55), indicating that the β-ratio is the main factor determining measurement sensitivity, and the impact of cone angles is minor.

While it might have been anticipated that the minimal (P_1-P_2) for ISO-5167R would be observed compared to the other cases, it showed the highest value as it has the smallest convergent cone angle (7°). Two possible reasons for the highest measurement sensitivity could be its long length between points 1 and 2 and the influence of strong reversed flow at the divergent section on the flow at the throat section.

5. Discussion

The mesh independence study revealed that reliable and converged results could be obtained using a mesh size of 0.06 mm at the wall. A non-dimensional distance (Y^+) of up to five was used for the study, adhering to the recommendations of previous studies [6,24]. It was found that the differences between the computational and experimental pressures were within an acceptable range. Although some cases showed greater measured pressure loss compared to computational values, and in other cases, the measured pressure loss was less (see Table 2), overall, the computational modelling performed reasonably well. The maximum experimental uncertainty was estimated to be 6.5 %, and the maximum difference between computational and experimental results was 5 %. Although the results are acceptable, there is still room for improvement. The maximum difference of 5 % between computational and experimental results can be attributed to various factors, such as the absence of pressure tapping points in the model, as noted by Reader-Harris et al. [29], insufficient information on the roughness profile, uncertainty of turbulence intensity in the flow, assumption of a uniform pressure at the downstream pressure tapping point, and assumption of fully developed flow at the inlet. Measuring the turbulence intensity at least at the entrance and the velocity and pressure profiles at the boundaries would also be beneficial. Incorporating measured velocity and pressure profiles at the boundaries and using actual turbulence intensity is expected to reduce the discrepancy between experimental and computational results. In addition, several improvements can be considered to enhance the accuracy of experimental results, such as regulating the room temperature, using a larger measurement tank with automated volume measurement, and employing more precise pressure gauges with a higher precision than 10 Pa.

When comparing the permanent pressure loss of ISO-5167 (0.31 kPa) with that of SVD4 Venturi meters (0.38 kPa), which have the same β-ratio of 0.55, the impact of convergent and divergent cone angles on permanent pressure loss can be evaluated. SVD4 (10°/10°) had a smaller convergent cone angle than ISO-5167 (21°/7°) but a larger divergent cone angle. However, the permanent pressure loss for ISO-5167 (0.31 kPa) was about 23 % less than that of SVD4 (0.38 kPa), suggesting a greater impact of the divergent cone angle on energy loss compared to the convergent cone angle for low Reynolds number turbulent flow. Thus, the study confirms that the divergent cone angle has a higher impact on Venturi meter performance than the convergent cone angle for Reynolds numbers of ≈34,000. This finding is consistent with the results reported in the literature for flows at higher Reynolds numbers.

This study identified two types of reversed flow in the Venturi meters: the ones originating at the start of the divergent section and those appearing at the middle or end of the divergent section. The strength of the first type increases as the Reynolds number increases, and they still exist at Reynolds numbers as low as 5,000, albeit weaker. The high divergent cone angle contributes to this type of reversed flow. The second type of reversed flow appears at the middle or end of the divergent section. These are weak reverse flows, and their strength reduces as the Reynolds number increases, eventually disappearing at a specific Reynolds number. The lack of sufficient momentum of the flow to overcome the reversed pressure gradient at the boundary layer of the divergent section appears to be the reason for this type of reversed flow.

The ISO-5167 Venturi has consistently demonstrated superior performance to other Venturis for unidirectional flows at Reynolds numbers between ≈34,000 and 200,000. It shows the lowest ζ ratio, no reverse flow at any point within the Venturi, excellent measurement sensitivity, and low permanent pressure loss. Previous studies have also demonstrated its strong performance at higher Reynolds numbers. However, at very low Reynolds numbers, such as 5,000, the ISO-5167 Venturi has exhibited a weak reverse flow. This characteristic may render it unsuitable in very low Reynolds number turbulent flows. However, this study did not find an alternative Venturi at very low Reynolds turbulent flows.

This study did not find a suitable symmetrical Venturi for flows with Reynolds numbers less than 100,000 for bidirectional flows. Several Venturis evaluated in the study exhibited strong reverse flow across the

Table 4
The performance of SVD4 and ISO-5167 Venturis at conventional and reversed flow direction and different Reynolds numbers.

Venturi (Convergent angle/divergent angle)	Flow direction	Re	Measurement sensitivity (kPa)	Permanent pressure loss (kPa)	ζ	Cd
ISO-5167 (21°/7°)	Conventional	50,000	5.19	0.67	0.13	0.98
ISO-5167 (21°/7°)	Conventional	100,000	20. 63	2.35	0.11	0.98
ISO-5167 (21°/7°)	Conventional	200,000	82.04	8.29	0.10	0.99
SVD4 (10°/10°)	Conventional	50,000	5.26	0.85	0.16	0.97
SVD4 (10°/10°)	Conventional	100,000	20.87	3.04	0.15	0.98
SVD4 (10°/10°)	Conventional	200,000	82.88	10.72	0.13	0.98
ISO-5167 (7°/21°)	Reversed	50,000	5.33	2.26	0.44	0.96
ISO-5167 (7°/21°)	Reversed	100,000	21.07	8.26	0.39	0.97
ISO-5167 (7°/21°)	Reversed	200,000	83.37	27.55	0.33	0.98

entire Reynolds number range. The best-performing symmetrical Venturi was SVD4, which can only be employed at Reynolds numbers greater than 100,000 as it exhibited reverse flow at the end of the divergent section for flows with Reynolds numbers less than 100,000.

The study suggests that the ISO-5167 Venturi is are the optimal choice for applications where flow is in the conventional direction. However, this Venturi showed a strong reverse flow in the opposite direction. In those conditions, the Venturi SVD4 is recommended. The size and strength of the reversed flow are weak for Reynolds numbers less than 100,000, and no reversed flow is observed at Reynolds numbers greater than 100,000 for SVD4. Substituting ISO-5167 with SVD4 can potentially save energy for bi-directional flow applications. To estimate the energy savings in an application with 50 % flow in one direction and 50 % in the opposite, Table 5 is provided based on the permanent pressure losses presented in Tables 2 and 3.

In Table 5, the calculation of the percentage of energy saving by replacing the ISO-5167 Venturi with the SVD4 Venturi for bi-directional applications utilised the permanent pressure losses, which directly and linearly impact energy consumption. For instance, at $Re \approx 34{,}000$ for the conventional flow direction, replacing ISO-5167 with SVD4 resulted in 28 % more energy consumption ((0.41–0.32)/0.32). However, for the opposite flow direction, it led to 71 % less energy usage ((1.41–0.41)/1.41). Therefore, there was a total energy saving of 43 % (71 % - 28 %). Similar calculations of the energy saving percentage were conducted at other Reynolds numbers, revealing a slight decrease in energy saving at higher Reynolds numbers.

Table 5
Energy savings for bidirectional applications (50 % in the conventional direction, 50 % in the opposite direction) between SVD4 and ISO-5167 Venturi meters at different Reynolds numbers.

Venturi	Re = 34,000	Re = 50,000	Re = 100,000	Re = 200,000
SVD4: Permanent pressure loss in the conventional direction (kPa)	0.41	0.85	3.04	10.72
SVD4: Permanent pressure loss in the opposite direction (kPa)	0.41	0.85	3.04	10.72
ISO-5167: Permanent pressure loss in the conventional direction (kPa)	0.32	0.67	2.35	8.29
ISO-5167: Permanent pressure loss in the opposite direction (kPa)	1.41	2.26	8.26	27.55
Energy saving percentage in the conventional direction if SVD4 is used	-28 %	-27 %	-30 %	-30 %
Energy saving in the opposite direction (%) if SVD4 is used	71 %	62 %	63 %	61 %
Total energy saving (%) if SVD4 is used	43 %	35 %	33 %	31 %

6. Conclusion

This study aimed to identify suitable geometries for single-phase isothermal incompressible low Reynolds number turbulent flows considering high measurement sensitivity, low energy loss and low relative pressure loss. The scope of the research was limited to an asymmetric Venturi manufactured to the ISO-5167 standard and six symmetrical Venturi meters with β-ratios of 0.4 and 0.55 and cone angles of 10°, 20° and 40°.

The computational analysis conducted in this study demonstrates that reliable results, with residuals of less than 10^{-8} for the continuity equation, pressure, and velocity components, can be achieved using $Y^{+} < 5$. The results are consistent with previous studies on flow at higher Reynolds numbers. The study suggests two types of reversed flow within Venturis: those that originate at the start of the divergent section and persist at other Reynolds numbers and those that start at the end of the divergent section and disappear or become weaker at higher Reynolds numbers. The findings confirm the superior performance of the ISO-5167 Venturi for unidirectional flow applications at Reynolds number greater than ≈34,000. A symmetrical Venturi with a β-ratio of 0.55 and cone angles of 10° exhibited good performance for bi-directional flows and a Reynolds number greater than ≈100,000. This Venturi can save up to 43 % energy compared to the ISO-5167 Venturi in low Reynolds number flow applications without compromising the measurement sensitivity.

Funding sources

This research received no specific grant from funding agencies in the public, commercial, or not-for-profit sectors.

CRediT authorship contribution statement

Ahmad Sharifian: Writing – review & editing, Writing – original draft, Validation, Supervision, Software, Methodology, Formal analysis, Data curation. **Keith Wells:** Writing – review & editing, Writing – original draft, Validation, Software, Resources, Methodology, Formal analysis, Data curation, Conceptualization.

Declaration of competing interest

The authors declare that they have no known competing financial interests or personal relationships that could have appeared to influence the work reported in this paper.

Data availability

Data will be made available on request.

References

[1] R.C. Baker, Flow Measurement handbook: Industrial designs, Operating principles, performance, and Applications, 2nd edition, Cambridge University Press, New York, NY, 2016, pp. 10013–12473. USA.
[2] M. Reader-Harris, Orifice Plates and Venturi Tubes, Springer International Publishing, Basel, Switzerland, 2015, pp. 13–14.
[3] International Organization for Standardization, 2003. Measurement of fluid flow by means of pressure differential devices inserted in circular cross-section conduits running full — Part 4: Venturi tubes. Viewed 14 January 2023. https://www.iso.org/standard/30192.html.
[4] A.R. Kaladgi, A. Mukhtar, A. Afzal, M. Kareemullah, M.K. Ramis, Numerical investigation of beta ratio and reynolds number effect on coefficient of discharge of Venturimeter, in: IOP Conference Series: Materials Science and Engineering 884, IOP Publishing, 2020 012116.
[5] R.W. Miller, Flow Measurement Engineering Handbook, 3rd edn, McGraw-Hill, New York, 1996.
[6] Z.B. Sharp, M.C. Johnson, S.L. Barfuss, Optimising the ASME Venturi recovery cone angle to minimise head loss, J. Hydraul. Eng. 144 (1) (2018) 04017057.
[7] M.M. Ghorani, B. Karimi, S.M. Mirghavami, Z. Saboohi, A numerical study on the feasibility of electricity production using an optimised wind delivery system (Invelox) integrated with a Horizontal axis wind turbine (HAWT), Energy 268 (2023) 126643.
[8] S. Siahpour, F.N. Khakiani, V. Fazlollahi, A. Golozar, F.A. Shirazi, Morphing omni-directional panel mechanism: a novel active roof design for improving the performance of the wind delivery system, Energy 217 (2021) 119400.
[9] M. Anbarsooz, M. Amiri, I. Rashidi, A novel curtain design to enhance the aerodynamic performance of Invelox: a steady-RANS numerical simulation, Energy 168 (2019) 207–221.
[10] D. Allaei, D. Tarnowski, Y. Andreopoulos, INVELOX with multiple wind turbine generator systems, Energy 93 (2015) 1030–1040.
[11] T.K. Patra, S. Mukherjee, P.N. Sheth, Process simulation of hydrogen rich gas production from producer gas using HTS catalysis, Energy 173 (2019) 1130–1140.
[12] S.S. de la Fuente, U. Larsen, R. Pawling, I.G. Kerdan, A. Greig, R. Bucknall, Using the forward movement of a container ship navigating in the Arctic to air-cool a marine organic Rankine cycle unit, Energy 159 (2018) 1046–1059.
[13] P.A. Sleigh, C.J. Noakes, CIVE1400: boundary layer theory, an Introduction to Fluid Mechanics, School of Civil Engineering, University Of Leeds, UK (2009). Viewed 10 April 2023, http://www.sleigh-munoz.co.uk/fluidsnotes/FluidsLevel1/Unit04/T2.html.

[14] P. Liu, H. Liu, Y. Yang, M. Wang, Y. Sun, Comparison of design methods for negative pressure gradient rotary bodies: a CFD study, PLoS ONE 15 (1) (2020) e0228186.
[15] E.M. Sparrow, J.P. Abraham, W.J. Minkowycz, Flow separation in a diverging conical duct: effect of Reynolds number and divergence angle, Int. J. Heat Mass Transf. 52 (13–14) (2009) 3079–3083.
[16] E. Fried, I.E. Idelchik, Flow resistance: a Design Guide For Engineers, Routledge, New York, 2017, https://doi.org/10.1201/9780203755754.
[17] White, F.M., 2006. Fluid Mechanics, 6th edn. Series in Mechanical Engineering, McGraw Hill.
[18] C. Sanghani, D. Jayani, Optimisation of Venturimeter geometry for minimum pressure drop using CFD analysis, Recent JCARME Numer. Model. 10 (2016) 31–35. Vol,.
[19] J. Tu, G.H. Yeoh, C. Liu, Computational fluid dynamics: a practical approach, Butterworth-Heinemann (2018).
[20] R. Sherrard, Ansys fluent - tips, tricks, and troubleshooting', Nimbix Supercomputing Suite (2020). Viewed 10 April 2023, https://support.nimbix.net/hc/en-us/articles/360044738671-ANSYS-Fluent.
[21] ANSYS, 2013. ANSYS Fluent Theory Guide 15.0. ANSYS, Canonsburg, PA, 33.
[22] D. Valero, D.B. Bung, B.M. Crookston, Energy dissipation of a Type III basin under design and adverse conditions for stepped and smooth spillways, J. Hydraul. Eng. 144 (7) (2018) 04018036.
[23] C. Torres, D. Borman, A. Sleigh, D. Neeve, Application of three-dimensional CFD VOF to characterise free-surface flow over trapezoidal labyrinth weir and spillway, J. Hydraul. Eng. 147 (3) (2021) 04021002.
[24] Versteeg, H.K. and Malalasekera, W., 2007. An introduction to computational fluid dynamics: the finite volume method. Pearson education.
[25] Roache, P.J., 1994. Perspective: a method for uniform reporting of grid refinement studies.
[26] M. Lee, G. Park, C. Park, C. Kim, Improvement of grid independence test for computational fluid dynamics model of building based on grid resolution, Adv. Civil Engineering (2020) 1–11, 2020.
[27] M. Malvoni, C. Baglivo, P.M. Congedo, D. Laforgia, CFD modeling to evaluate the thermal performances of window frames in accordance with the ISO 10077, Energy 111 (2016) 430–438.
[28] Y. Han, X. Wang, H. Sun, G. Zhang, L. Guo, J. Tu, CFD simulation on the boundary layer separation in the steam ejector and its influence on the pumping performance, Energy 167 (2019) 469–483.
[29] M.J. Reader-Harris, N. Barton, W.C. Brunton, J.J. Gibson, D. Hodges, I. G. Nicholson, P. Johnson, The discharge coefficient and through-life performance of Venturi tubes, in: Proceedings of 18th North Sea Flow Meas Workshop, Gleneagles, paper 5, 2000.